A reversible molecular valve

Thoi D. Nguyen, Hsian-Rong Tseng, Paul C. Celestre, Amar H. Flood, Yi Liu, J. Fraser Stoddart*, and Jeffrey I. Zink*

Department of Chemistry and Biochemistry and California NanoSystems Institute, University of California, 405 Hilgard Avenue, Los Angeles, CA 90095

Communicated by M. Frederick Hawthorne, University of California, Los Angeles, CA, May 25, 2005 (received for review January 27, 2005)

In everyday life, a macroscopic valve is a device with a movable control element that regulates the flow of gases or liquids by blocking and opening passageways. Construction of such a device on the nanoscale level requires (*i*) suitably proportioned movable control elements, (*ii*) a method for operating them on demand, and (*iii*) appropriately sized passageways. These three conditions can be fulfilled by attaching organic, mechanically interlocked, linear motor molecules that can be operated under chemical, electrical, or optical stimuli to stable inorganic porous frameworks (i.e., by self-assembling organic machinery on top of an inorganic chassis). In this article, we demonstrate a reversibly operating nanovalve that can be turned on and off by redox chemistry. It traps and releases molecules from a maze of nanoscopic passageways in silica by controlling the operation of redox-activated bistable [2]rotaxane molecules tethered to the openings of nanopores leading out of a nanoscale reservoir.

controlled release | nanomachine | nanovalve

Progress in designing and synthesizing nanovalves that control access to and from the pores in inorganic materials is proceeding apace. Our previous work (1), involving the fabrication of pseudorotaxane-derivatized, nanostructured thin films, demonstrated a reusable but irreversible nanovalve that acts like a cork in a bottle, opening the orifices of a two-dimensional hexagonal array of cylindrical pores and allowing the contents to spill out. Other examples, using more traditional control mechanisms, have been described in the literature. Based on photodriven motions involving cis-trans isomerizations of N=N double bonds, azobenzenes tethered to the walls of the nanoporous membranes function (2) as a regulatory mechanism for mass transport through the channels of nanoporous materials. Using the intermolecular dimerization of tethered coumarins, dimers act (3, 4) as a net to control the access to and from the pores of derivatized MCM-41 upon photoactivation and subsequent dedimerization. Chemically linked CdS nanoparticles on derivatized mesoporous silica nanospheres function (5) as caps to control the release of chemicals from the pores. Although, in the latter two examples, covalent bonds are broken to control the release of the pore's contents, the first instance is one in which a change in a molecule's configuration, and hence shape, does the trick. Based on pH-sensitive intermolecular hydrogen bonds between poly(ethyloxazoline) and poly(methacrylic acid), a polymer gel can be eroded electrically, leading to the release of a trapped insulin load (6). A heat-responsive polymer, poly(*N*-isopropylacrylamide) (PNIPAAm), has also been used (7) as the source of hindrance at the pores' orifices to modulate the transport of solute, albeit in an irreversible fashion. By using monolithic copolymers to define pores with tunable sizes ranging from tens to thousands of nanometers, PNIPAAm has been shown (8) to behave as a reversible valve in microfluidic chips. The electrochemical corrosion of gold into soluble gold chloride is the mechanism exploited for the use of a gold membrane in microelectromechanical systems to cover etched silicon reservoirs filled with drugs. Upon application of a positive potential, electrochemical corrosion of the gold membranes releases the drugs (9–11). Porous silica has also been used for uncontrolled release of drugs (12).

Molecular machines (13–17) are attractive systems for deployment in the development of nanovalves on account of their abilities to be customized and optimized for a range of functions at the nanoscale. The attachment of supramolecular and molecular machines to nanoparticles has been achieved in a number (18–21) of different classes of systems. In our most recent research, described in this report, the movable control element that has been used to control the flow of molecules in a nanovalve is a bistable, redox-controllable [2]rotaxane $\mathbf{R}^{4+}$, shown in Fig. 1. Mechanically interlocked molecules of this kind (22, 23) have been studied of late for their ability to be switched either chemically or electrochemically in solution (24), as a Langmuir–Blodgett monolayer on a silica surface (25), in a solid-state polymer matrix (26), as a self-assembled monolayer on gold (27), and as a monolayer sandwiched between two electrodes in crossbar memory devices (28, 29). In $\mathbf{R}^{4+}$, the movable part of the molecule is the tetracationic cyclophane, cyclobis(paraquat-*p*-phenylene) ($CBPQT^{4+}$) component that can be induced to move between two different recognition sites or stations on the dumbbell component. In its ground state, the $CBPQT^{4+}$ ring prefers to encircle the tetrathiafulvalene (TTF) station, rather than the dioxynaphthalene (DNP) one, which is separated from the TTF station by an oligoethyleneglycol chain incorporating a rigid terphenylene spacer. Because the stabilization energy between $CBPQT^{4+}$ and TTF is >2 kcal/mol more than that between $CBPQT^{4+}$ and DNP, it follows that, in >95% of the molecules, the $CBPQT^{4+}$ ring encircles the TTF station. Two-electron oxidation of the TTF station with $Fe(ClO_4)_3$ to give the TTF^{2+} dication destabilizes its interaction (coulombic repulsion) with the $CBPQT^{4+}$ ring, which moves to the DNP station in its electromechanical excited state. The preference for the $CBPQT^{4+}$ ring to encircle the DNP station instead of the TTF^{2+} dication is even greater on account of the large difference (≈8 kcal/mol, at least) in their stabilization energies. Reduction of the TTF^{2+} dication back to the neutral TTF unit by ascorbic acid heralds the return of the $CBPQT^{4+}$ ring to the TTF station in a thermally activated process (24).

Experimental Procedures

General Methods. Chemicals were purchased from Aldrich and used as received. 3-isocyanatopropyltriethoxysilane (3-ICPES) was purchased from Gelest (Morrisville, PA) and used after distillation. Rhodamine B was purchased from Lambda Physik (Acton, MA) and used as received. Tris(2,2′-phenylpyridyl)iridium(III) [$Ir(ppy)_3$]was a gift from Mark Thompson (University of Southern California, Los Angeles). The bromide **1** (30), 4-hydroxy-3,5-diisopropyl-benzaldehyde (**5**) (31), Grignard reagent **8** (30), tosylate **10** (30), and a,a′-[1,4-phenylenebis(methylene)]bis(4,4′-bipyridium) bis(hexafluorophosphate) (**12**·$2PF_6$) (32) were all prepared according to procedures described in the literature. Solvents were dried following methods described in ref. 33. All reactions were

Freely available online through the PNAS open access option.

Abbreviations: $CBPQT^{4+}$, cyclobis(paraquat-*p*-phenylene); TTF, tetrathiafulvalene; DNP, dioxynaphthalene; ICPES, isocyanatopropyltriethoxysilane; $Ir(ppy)_3$, Tris(2,2′-phenylpyridyl)iridium(III).

*To whom correspondence may be addressed. E-mail: stoddart@chem.ucla.edu or zink@chem.ucla.edu.

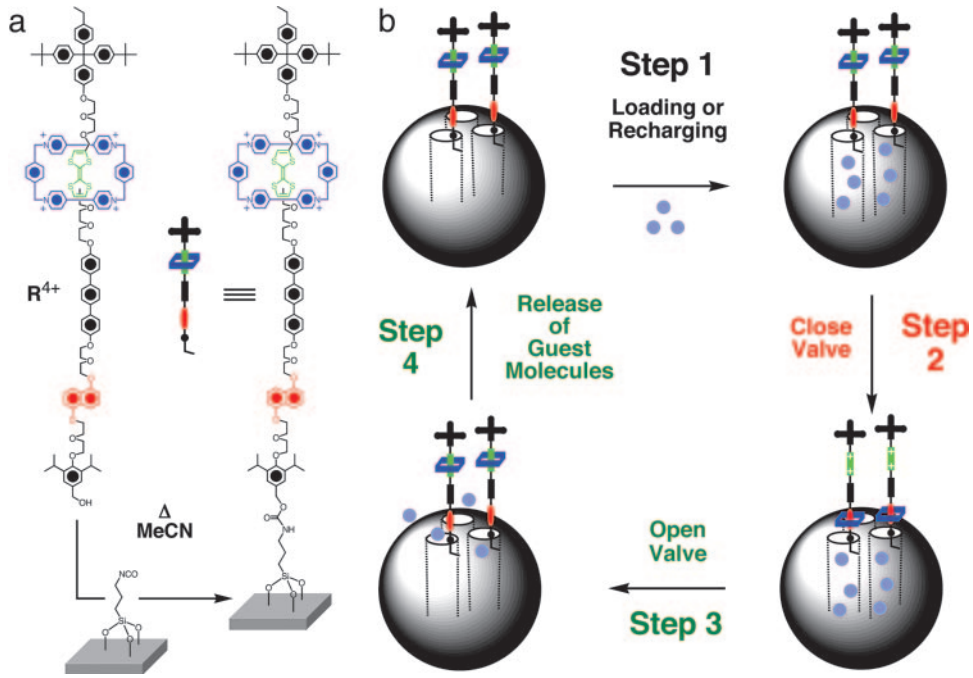

Fig. 1. Graphical representations of the surface attachment of bistable rotaxanes to silica particles along with a cycle for loading and release of guest molecules. (*a*) The structural formula of the bistable [2]rotaxane $\mathbf{R}^{4+}$ and the procedure used for tethering $\mathbf{R}^{4+}$ to the surface of mesoporous silica particles. (*b*) The proposed mechanism for the operation of the nanovalve. The moving part of the molecular valve is a $CBPQT^{4+}$ ring (blue), which shuttles between a TTF station (green) and a DNP station (red) under redox control. The openings of the cylindrical pores on the silica are blocked by the $CBPQT^{4+}$ ring when the valve is closed. Guest molecules (turquoise spheres) are loaded in Step 1 by diffusion into the open pores when the $CBPQT^{4+}$ ring is located on the TTF station. The valve is closed in Step 2 by oxidation of the TTF unit to its dication, causing the $CBPQT^{4+}$ ring to move to the DNP station, which is much closer to the openings of the pores. The valve can be opened (Step 3) by adding ascorbic acid to reduce the TTF dication back to its neutral state, whereupon the $CBPQT^{4+}$ ring moves back from the DNP station to be relocated around the much more π electron-rich TTF station, releasing the guest molecules in Step 4. The valve is ready for recharging (i.e., returning to Step 1). Thus, the valve can be closed and opened reversibly. The silica particles are not drawn to scale, and only a few of the ordered pores are shown.

carried out under an anhydrous argon/nitrogen atmosphere. TLC was performed on aluminum sheets coated with silica-gel 60F (Merck 5554). The plates were inspected by UV light and, if required, developed in I_2 vapor. Column chromatography was carried out by using silica-gel 60 (Merck 9385, particle size 230–400 mesh). Melting points were determined on an Electrothermal 9100 melting point apparatus and are uncorrected. All ^1H and ^{13}C NMR spectra were recorded on either an ARX500 (Bruker, Billerica, MA) (500 and 125 MHz, respectively) or an Avance500 (Bruker) (500 and 125 MHz, respectively), using residual solvent as the internal standard. Samples were prepared by using $CDCl_3$, CD_3COCD_3, or CD_3CN purchased from Cambridge Isotope Laboratories (Cambridge, MA). All chemical shifts are quoted using the δ scale, and all coupling constants (J) are expressed in hertz. Fast atom bombardment mass spectra were obtained by using a ZAB-SE mass spectrometer equipped with a krypton primary atom beam, using a *m*-nitrobenzyl alcohol matrix. X-ray diffraction patterns of MCM-41 were recorded on a locally fabricated powder x-ray diffractometer equipped with a 3-kW sealed-tube generator Cu Kα x-ray source, graphite monochromator. Particle sizes were measured from SEM images (JEOL 4700J). The release of dyes from the functional material was monitored by using a fluorolog FL3–22 (ISA Spex, Jobin Yvon, Longjumeau, France) equipped with an ozone-free xenon lamp.

Synthesis of [2]Rotaxane R·4PF$_6$ and Its Precursor, Dumbbell-Shaped Compound D. The routes used to synthesize the [2]rotaxane **R**·4PF$_6$ and its respective dumbbell-shaped compound **D** are outlined in Schemes 1 and 2. Using conventional alkylation reaction conditions (K_2CO_3/LiBr/[18]crown-6/MeCN), the bromide **1** was reacted with 4′-bromo(1,1′-biphenyl)-4-ol (**2**) to obtain the alcohol **3** in 92% yield. Subsequent tosylation of the alcohol **3** afforded the tosylate **4**, which was then treated with 4-hydroxy-3,5-diisopropyl-benzaldehyde (**5**) under the previously mentioned alkylation conditions to give the aldehyde **6** in 85% yield overall. The aldehyde **6** was converted to compound **7** by reduction ($NaBH_4$/MeOH), followed by a protection group step (3,4-dihydro-2*H*-pyran/*p*-toluenesulfonic acid (PTSA)/CH_2Cl_2). Without further purification, compound **7** was then reacted with the freshly prepared Grignard reagent **8** in the presence of $Pd(PPh_3)_4$. The resulting product was directly dissolved in a mixed solution (HCl/MeOH/CH_2Cl_2), where it underwent an HCl-catalyzed deprotection to give the diol **9** with an overall yield of 69% for the four steps starting from the aldehyde **6**.

The synthesis of the [2]rotaxane **R**·4PF$_6$ was completed (Scheme 2) by alkylating **9** with the tosylate **10** in MeCN in the presence of K_2CO_3, LiBr, and [18]crown-6 to afford the dumbbell-shaped compound **D** in 78% yield. The template-directed synthesis of the [2]rotaxane **R**·4PF$_6$ was accomplished by reacting **D**, 1,4-bis(bromomethyl)benzene (**11**), and the dicationic salt **12**·2PF$_6$ in dimethylformamide (DMF) at room temperature for 10 days. The [2]rotaxane **R**·4PF$_6$ was isolated in 52% yield as an analytically pure green solid after chromatography on silica gel, using a 1% NH_4PF_6 solution in Me_2CO as the eluent, followed by the addition of H_2O.

All compounds were fully characterized by mass spectrometry and ^1H NMR spectroscopy. In some instances, ^{13}C NMR spectra were also obtained. These details are provided in the supporting information, which is published on the PNAS web site.

Synthesis of MCM-41 and Surface Attachment of Bistable [2]Rotaxanes. Submicrometer-size spheres of MCM-41 are prepared according to procedures described in ref. 34. MCM-41 is char-

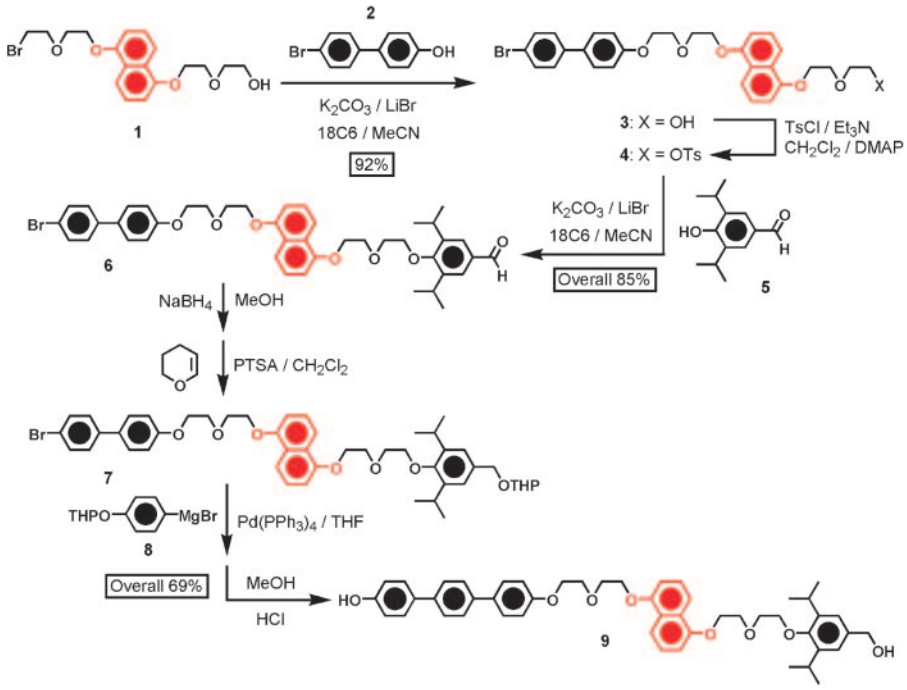

Scheme 1. Reaction scheme illustrating the synthesis of the dumbbell component **9**.

acterized by powder x-ray diffraction and scanning electron microscopy. Surfactant is removed by calcination at 823 K for 5 h. Surfactant removal is confirmed based on the shifting of the Bragg peaks. MCM-41 is derivatized with ICPES by using a gas-phase reaction between MCM-41 and ICPES-toluene solution (35). The reaction is run for 12 h under an inert atmosphere. The ICPES-derivatized material is soaked in PhMe for 1 day to wash away adsorbed ICPES. The material is then dried under reduced pressure. Refluxing the ICPES-modified MCM-41 in an MeCN solution of the [2]rotaxane **R**·$4PF_6$ for 10 h under inert atmosphere affords the [2]rotaxane-MCM-41. The dumbbell component **D** of the [2]rotaxane is tethered to the mesoporous silica by refluxing the ICPES-modified MCM-41 in a $CHCl_3$ solution of the dumbbell **D** for 12 h. Extensively washed material is tested for the presence of [2]rotaxane or the dumbbell component, based on DNP luminescence of the powder material

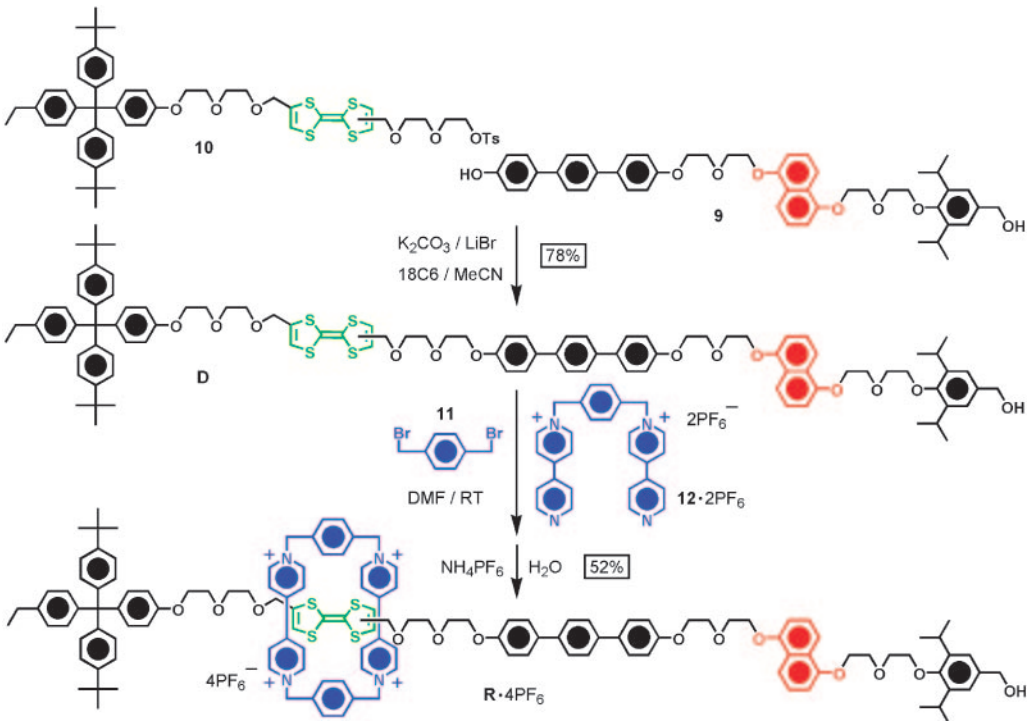

Scheme 2. Reaction scheme illustrating the synthesis of the bistable [2]rotaxane **R**·$4PF_6$.

(excitation wavelength = 295 nm). The loading of derivatized MCM-41 with guest molecules is achieved by soaking the derivatized material in solutions of the guest molecules with the concentrations ranging from 0.4 to 0.5 mM. Approximately two equivalents of $Fe(ClO_4)_3 \cdot 6H_2O$ in MeCN (the amount of $Fe(ClO_4)_3 \cdot 6H_2O$ used is estimated based on the amount of [2]rotaxane that serves as the limiting reagent) is added to the loaded material. The loaded-and-closed material is washed with appropriate solvents until the filtrate does not show any trace of guest molecules. The loaded-and-closed material is then confirmed to be in the closed coconformation based on DNP luminescence. The functional material is then ready for controlled release study.

Results and Discussion

The nanoscale passageways that will contain trapped molecules are prepared by surfactant-directed self-assembly to yield ordered arrays of channels in sol-gel-derived silica (36–38). The material used in this investigation (namely, MCM-41) consists of roughly spherical silica particles prepared by sol-gel methods with an average diameter of 620 nm as verified by SEM that are templated by cetyltrimethylammonium bromide to produce (34, 39, 40) pores with a diameter of 1.5–2.0 nm. The highly ordered pores form a two-dimensional hexagonal structure with a lattice spacing of 3.6 nm as measured by x-ray diffraction. The surfactant is removed by calcination for 5 h at 550°C, yielding a highly porous material with a pore volume of 0.77 $cm^3 \cdot g^{-1}$.

Coupling [2]rotaxane $\mathbf{R}^{4+}$ to the calcined mesoporous silica was accomplished by first derivatizing the silica with ICPES, which serves as a linker between the hydroxyl-terminated stopper on the [2]rotaxane and the silicate surface. ICPES is bonded (35, 41) to the calcined material by using a vapor-phase reaction. On account of its relatively small size, ICPES can cover the outer surface of the MCM-41 particles and the interior of the pores. The hydroxyl group on the stopper of $\mathbf{R}^{4+}$ reacts (42) with the isocyanate in refluxing acetonitrile (MeCN) to form a carbamate linkage. Unlike ICPES, the relatively large size of $\mathbf{R}^{4+}$ prevents it, we believe, from penetrating deep inside the pore. Confirmation of the attachment of the [2]rotaxane to the surface of the washed material was obtained by fluorescence spectroscopic observation of the DNP station. In this initially derivatized silica, the valve will be open because the coupling places the free DNP station closer to the silica, and the bulky $CBPQT^{4+}$ ring is associated with the much more distant and occupied TTF station.

The filling of the pores with guest molecules is carried out by soaking the derivatized silica in a solution containing the guest compound and exploiting the concentration gradient between the highly accessible pores and the solution (12, 43). After this diffusion step has been completed, approximately two equivalents of $Fe(ClO_4)_3$ are added, thus causing (22) the $CBPQT^{4+}$ ring to move from the TTF to the DNP station and block the pores (2).

To monitor the confinement and release of the guest molecules, luminescent compounds that do not react with the redox reagents were chosen. Both a neutral compound, $Ir(ppy)_3$, in PhMe:EtOH (1:1) solution and a cationic compound, rhodamine B, in MeCN solution were studied. Rhodamine B, tetraethyl-3,6-diaminofluoran, is a laser dye and biological stain with a fluorescent band maximum at 580 nm. The luminescent guest molecules are loaded into the pores by soaking the [2]rotaxane-modified MCM-41 in the dye solution and then filtrating and drying. The selection of the solvent for the loading and release processes is based on the solubility of the released molecules. $Ir(ppy)_3$ is a highly luminescent molecule ≈1 nm in diameter, with an emission band maximum at 506 nm.

To close the valve and confine the guest molecules, two to three equivalents of $Fe(ClO_4)_3$ in solution were added to the dry material and then filtrated. The material was washed with the appropriate solvent until no spectroscopic trace of the guest molecule in the solution was observed. This process washes away surface adsorbed molecules. The confinement of the guest molecules in the closed pores of the silica was verified by their luminescence spectra when the solid material was excited. These guest molecules are confined and could not be washed away. The shuttling of the $CBPQT^{4+}$ ring from the TTF station to the DNP station was confirmed by the decrease in luminescence (≈4-fold) of the DNP ring system upon addition of $Fe(ClO_4)_3$. The naphthalene emission of the DNP ring system is quenched by the tetracationic cyclophane when it moves to that station and closes the valve.

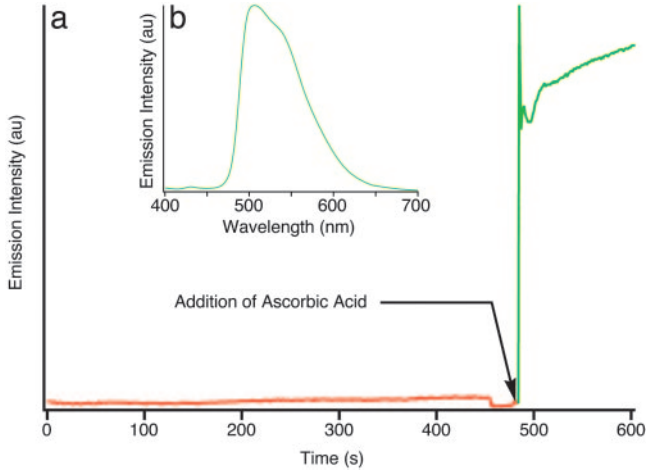

Fig. 2. Fluorescence data demonstrating the controlled release of the $Ir(ppy)_3$ guest molecules from the nonovalve. (*a*) Release of the $Ir(ppy)_3$ molecules from the pores can be monitored by luminescence spectroscopy. When the valve is opened by reduction of the TTF^{2+} dication with ascorbic acid, the luminescence of the solution increases rapidly. (*b*) The visible spectrum of the released $Ir(ppy)_3$ molecules is shown.

The release of $Ir(ppy)_3$ is measured by monitoring (Fig. 2) the emission spectrum in the solution above the solid MCM-41. The functional material is placed in a cell holder, such that only the solution is exposed to excitation light. The luminescence of $Ir(ppy)_3$ in solution at 506 nm is monitored over time. Before the valve is opened, a flat baseline is obtained. This flat baseline attests to the absence of leakage through the closed valve. Addition of ascorbic acid opens the valve. An immediate and fast increase in emission intensity is observed, showing that some of the guest molecules are released from the pores in the solid state and escape into solution.

It is important to verify (29) that the observed phenomena involving molecular machines is molecular in origin and that it is not a result of an artifact of the conditions. The operation of the valve itself can be monitored (Fig. 3) directly by following the luminescence of the DNP station. When the valve is closed, the luminescence is quenched by the $CBPQT^{4+}$ ring. After addition of ascorbic acid, the $CBPQT^{4+}$ ring moves to the TTF station, and the naphthalene intensity increases 4-fold. This spectroscopic result shows that shuttling of tetracationic cyclophane from the DNP to the TTF station occurs in concert with the release process.

As a means to determine whether electrostatic interactions between the guest molecules and the functional material affect the operation of the valve, a cationic molecule, rhodamine B, was chosen as a probe and guest molecule. The controlled release of rhodamine B can be measured in the same manner as that of $Ir(ppy)_3$ guest molecules. Before release, the emission baseline at 580 nm is flat. But, upon addition of ascorbic acid, the

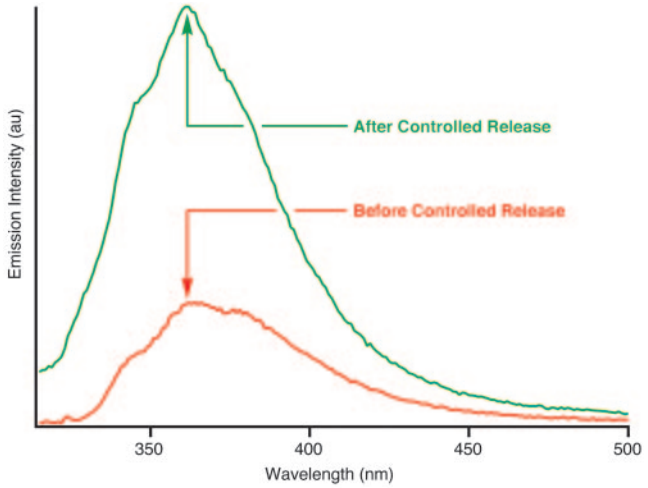

Fig. 3. Naphthalene luminescence is used to monitor the operation of the valve. In its closed state when the $CBPQT^{4+}$ ring encircles the DNP station, naphthalene luminescence is quenched by the tetracatronic cyclophane. When the valve is in its open state when the $CBPQT^{4+}$ ring encircles the TTF station, the luminescence intensity of the naphthalene ring system in the DNP station increases 4-fold.

emission intensity increases sharply (Fig. 4*a*). The emission of naphthalene in the valve itself increases 4-fold, indicating that the $CBPQT^{4+}$ ring moves from the DNP station to the TTF station. As shown in Figs. 2 and 4, the releases of both $Ir(ppy)_3$ and rhodamine B are similar, indicating that charged molecules do not disrupt the operation of the valve.

To confirm the role of the $CBPQT^{4+}$ ring motion as the crucial component of the nanovalve operation, the dumbbell compound **D** lacking the ring present in $\mathbf{R}^{4+}$ itself has also been attached to silica particles in exactly the same manner as already described for the [2]rotaxane. The use of the dumbbell component of a rotaxane as a control for the verification of molecular motion in the latter has been used successfully in a range of systems, including switchable monolayers (25, 27), molecular electronics (16, 28, 29), and in molecule-based nanoelectromechanical systems (44). This control system was then loaded with rhodamine B, as outlined above for $\mathbf{R}^{4+}$, and placed in the solvent. The guest molecules leak immediately into solution. Also, no further increase in emission intensity in solution occurs upon the addition of ascorbic acid. The guest molecules are not trapped, and hence the addition of ascorbic acid has no effect. The dumbbell **D** compound does not block the pores and hence does not prevent the escape of the guest molecules.

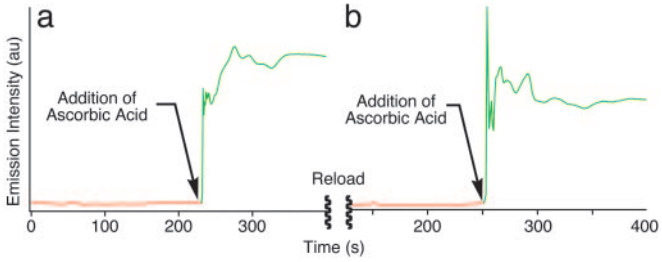

Fig. 4. Release of the rhodamine B guest molecules is monitored by following the luminescence intensity of the solution. (*a*) After the valve has been opened by reduction of the TTF^{2+} dication with ascorbic acid, the luminescence in solution increases rapidly. (*b*) More guest molecules can be loaded into the pores and the valve closed by oxidation of the TTF station and later released by another reduction with ascorbic acid.

The controllable shuttling of the $CBPQT^{4+}$ ring between the DNP and TTF sites makes the nanovalve operation fully reversible (1, 45). To demonstrate this reversible operation, a second batch of rhodamine B was loaded into the pores of the previously discharged rotaxane-modified MCM-41, and the valve was closed again by the addition of $Fe(ClO_4)_3$. The controlled release profile exhibits the same character as that from the first cycle (Fig. 4b). The 4-fold increase in the naphthalene emission after opening the valve of this recycled system shows the reversibility of the [2]rotaxane $\mathbf{R}^{4+}$, affording it the status of being an operational molecular-based, mechanical nanovalve.

It is reversible relative motion within interlocked molecules attached to nanostructured inorganic frameworks that forms the basis for a nanovalve. The rotaxane-modified MCM-41 constitutes a class of organic–inorganic hybrid nanoparticle that utilizes the mechanical movement within a mechanically interlocked molecule to control trapping and release of guest molecules. The valve is controlled by simple redox chemistry with mild redox reagents. This operational valve is a true molecular machine consisting of a solid framework with movable parts to accomplish (46) a specific task. In principle, photochemical or electrical energy could also be used to power and control the nanovalve. Although luminescent guest molecules were chosen for investigation by us in the beginning to establish proof of principle and establish the nanovalve action, future applications could include nanofluidic systems and the controlled release of drugs from implants with nanoscopic properties.

We thank Prof. M. Thompson for the gift of $Ir(ppy)_3$ and Prof. H. Monbouquette for use of the spectrofluorimeter. This work was supported by Nanoscale Interdisciplinary Research Team Grant NIRT ECS-0103559 from the National Science Foundation.

1. Hernandez, R., Tseng, H.-R., Wong, J. W., Stoddart, J. F. & Zink, J. I. (2004) *J. Am. Chem. Soc.* **126,** 3370–3371.
2. Liu, N., Dunphy, D. R., Atanassov, P., Bunge, S. D., Chen, Z., Lopez, G. P., Boyle, T. J. & Brinker, J. C. (2004) *Nano Lett.* **4,** 551–554.
3. Mal, N. K., Fujiwara, M. & Tanaka, Y. (2003) *Nature* **421,** 350–353.
4. Mal, N. K., Fujiwara, M., Tanaka, Y., Taguchi, T. & Matsukata, M. (2003) *Chem. Mater.* **15,** 3385–3394.
5. Lai, C.-Y., Trewyn, B. G., Jeftinija, D. M., Jeftinija, K., Xu S., Jeftinija, S. & Lin, V. S.-Y. (2003) *J. Am. Chem. Soc.* **125,** 4451–4459.
6. Kwon, I. C., Bae, Y. H. & Kim, S. W. (1991) *Nature* **354,** 291–293.
7. Fu, Q., Rama Rao, G. V., Ista, L. K., Wu, Y., Andrzejewski, B. P., Sklar, L. A., Ward, T. L. & Lopez, G. P. (2003) *Adv. Mater.* **15,** 1262–1266.
8. Luo, Q., Mutlu, S., Gianchandani, Y. B., Svec, F. & Fréchet, J. M. J. (2003) *Electrophoresis* **24,** 3694–3702.
9. Santini, J. T., Jr., Cima, M. J. & Langer, R. (1999) *Nature* **397,** 335–338.
10. Li, Y., Shawgo, R. S., Tyler, B., Henderson, P. T., Vogel, J. S., Rosenberg, A., Storm, P. B., Langer, R., Brem, H. & Cima, M. J. (2004) *J. Controlled Release* **100,** 211–219.
11. Shawgo, R. S., Voskerician, G., Duc, H. L. H., Li, Y., Lynn, A., MacEwan, M., Langer, R., Anderson, J. M. & Cima, M. J. (2004) *J. Biomed. Mater. Res.* **71A,** 559–568.
12. Xue, J. M. & Shi, M. (2004) *J. Controlled Release* **98,** 209–217.
13. Dietrich-Buchecker, C., Jimenez-Molero, M. C., Sartor, V. & Sauvage, J. P. (2003) *Pure Appl. Chem.* **75,** 1383–1393.
14. Barboiu, M. & Lehn, J.-M. (2002) *Proc. Natl. Acad. Sci. USA* **99,** 5201–5206.
15. van Delden, R. A., ter Wiel, M. K. J., de Jong, H., Meetsma, A. & Feringa, B. L. (2004) *Org. Biomol. Chem.* **2,** 1531–1541.
16. Flood, A. H., Ramirez, R. J. A., Deng, W.-Q., Muller, R. P., Goddard, W. A. & Stoddart, J. F. (2004) *Aust. J. Chem.* **57,** 301–322.
17. Hernandez, J. V., Kay, E. R. & Leigh, D. A. (2004) *Science* **306,** 1532–1537.
18. Fitzmaurice, D., Rao, S. N., Preece, J. A., Stoddart, J. F., Wenger, S. & Zaccheroni, N. (1999) *Angew. Chem. Int. Ed.* **38,** 1147–1150.
19. Ryan, D., Rao, S. N., Rensmo, H., Fitzmaurice, D., Preece, J. A., Wenger, S., Stoddart, J. F. & Zaccheroni, N. (2000) *J. Am. Chem. Soc.* **122,** 6252–6257.
20. Long, B., Nikitin, K. & Fitzmaurice, D. (2003) *J. Am. Chem. Soc.* **125,** 15490–15498.
21. Dulic, D., van der Molen, S. J., Kudernac, T., Jonkman, H. T., de Jong, J. J. D., Bowden, T. N., van Esch, J., Feringa, B. L. & van Wees, B. J. (2003) *Phys. Rev. Lett.* **91,** 207402.

22. Tseng, H.-R., Vignon, S. A. & Stoddart, J. F. (2003) *Angew. Chem. Int. Ed.* **42,** 1491–1495.
23. Kang, S., Vignon, S. A., Tseng, H.-R. & Stoddart, J. F. (2004) *Chem. Eur. J.* **10,** 2555–2564.
24. Flood, A. H., Peters, A. J., Vignon, S. A., Steuerman, D. W., Tseng, H.-R., Kang, S., Heath, J. R. & Stoddart, J. F. (2004) *Chem. Eur. J.* **24,** 6558–6561.
25. Huang, T. J., Tseng, H.-R., Sha, L., Lu, W., Brough, B., Flood, A. H., Yu, B.-D., Celestre, P. C., Chang, J. P., Stoddart, J. F. & Ho, C.-M. (2004) *Nano Lett.* **4,** 2065–2071.
26. Steuerman, D. W., Tseng, H.-R., Peters, A. J., Flood, A. H., Jeppesen, J. O., Nielsen, K. A., Stoddart, J. F. & Heath, J. R. (2004) *Angew. Chem. Int. Ed.* **43,** 6486–6491.
27. Tseng, H.-R., Wu, D., Fang, N. X., Zhang, X. & Stoddart, J. F. (2004) *Chem. Phys. Chem.* **5,** 111–116.
28. Luo, Y., Collier, P. C., Jeppesen, J. O., Nielsen, K. A., Delonno, E., Ho, G., Perkins, J., Tseng, H.-R., Yamamoto, T., Stoddart, J. F. & Heath, J. R. (2002) *Chemphyschem* **3,** 519–525.
29. Flood, A. H., Stoddart, J. F., Steuerman, D. W. & Heath, J. R. (2004) *Science* **306,** 2055–2056.
30. Tseng, H.-R., Vignon, S. A., Celestre, P. A., Perkins, J., Jeppesen, J. O., Di Fabio, A., Ballardini, R., Gangolfi, M. T., Venturi, M., Balzani, V. & Stoddart, J. F. (2004) *Chem. Eur. J.* **10,** 155–172.
31. Roth, B., Baccanari, D. P., Sigel, C. W., Hubbell, J. P., Eaddy, J., Kao, J. C., Grace, M. E. & Rauckman, B. S. (1988) *J. Med. Chem.* **31,** 122–129.
32. Ashton, P. R., Brown, G. R., Isaacs, N. S., Giuffrida, D., Kohnke, F. H., Mathias, J. P., Slawin, A. M. Z., Smith, D. R., Stoddart, J. F. & Williams, D. J. (1992) *J. Am. Chem. Soc.* **114,** 6330–6353.
33. Perrin, D. D. & Armarego, W. L. F. (1998) *Purification of Laboratory Chemicals* (Pergamon, New York).
34. Grun, M., Laner, I. & Unger, K. K. (1997) *Adv. Mater.* **9,** 254–257.
35. Haller, I. (1978) *J. Am. Chem. Soc.* **100,** 8050–8055.
36. Kresge, C. T., Leonowicz, M. E., Roth, W. J., Vartuli, J. C. & Beck, J. S. (1992) *Nature* **359,** 710–712.
37. Beck, J. S., Vartuli, J. C., Roth, W. J., Leonowicz, M. E., Kresge, C. T., Schmitt, K. D., Chu, C. T-W, Olson, D. H., Sheppard, E. W., McCullen, S. B., *et al.* (1992) *J. Am. Chem. Soc.* **114,** 10834–10843.
38. Monnier, A., Schuth, F., Huo, Q., Kumar, D., Margolese, D., Maxwell, R. S., Stucky, G. D., Krishnamurty, M., Petroff, P., Firouzi, A., *et al.* (1993) *Science* **261,** 1299–1303.
39. Kumar, D., Schumacher, K., du Fresne von Hohenesche, C., Grun, M. & Unger, K. K. (2001) *Colloids Surf.* **187–188,** 109–116.
40. Van Tendeloo, G., Lebedev, O. I., Collart, O., Cool, P. & Vansant, E. F. (2003) *J. Phys. Condens. Matter.* **15,** S3037–S3046.
41. Hertl, W. (1968) *J. Phys. Chem.* **72,** 1248–1253.
42. Entelis, S. G. & Nesterov, O. V. (1966) *Russ. Chem. Rev.* **35,** 917–929.
43. Doadrio, A. L., Sousa, E. M. B., Doadrio, J. C., Pariente, J. P., Izquierdo-Barba, I. & Vallet-Regi, M. (2004) *J. Controlled Release* **97,** 125–132.
44. Huang, T. J., Liu, Y., Flood, A. H., Brough, B., Bonvallet, P. A., Tseng, H.-R., Baller, M., Stoddart, J. F. & Ho, C.-M. (2004) *Appl. Phys. Lett.* **85,** 5391–5393.
45. Kim, K., Jeon, W. S., Kang, J.-K., Lee, J. W., Jon, S. Y., Kim, T. & Kim, K. (2003) *Angew. Chem. Int. Ed.* **42,** 2293–2296.
46. Katz, E., Sheeney-Haj-Ichia, L. & Willner, I. (2004) *Angew. Chem. Int. Ed.* **43,** 3292–3300.